# Metal-Assisted Ligand Oxidation: Synthesis and Characterization of Novel Manganese(III), Iron(III), and Nickel(II) Complexes

**Navamoney Arulsamy and Derek J. Hodgson***

Department of Chemistry, University of Wyoming, Laramie, Wyoming 82071

*Received April 21, 1994*[⊗]

The reaction of the ligand (2-pyridyl)bis(2-pyridylamino)methane (L1) in acetonitrile with nickel(II) perchlorate leads to the formation of the expected bis-chelated complex $[Ni(L1)_2](ClO_4)_2{\cdot}2CH_3CN$, but in the presence of air L1 reacts with manganese(II) and iron(II) perchlorate salts to form the novel mononuclear complexes $[M(L2)_2]ClO_4$ ($M = Mn^{III}$, $Fe^{III}$; L2 = (2-pyridyl)(2-pyridylamino)methanolato anion). The crystal structures of the complexes have been determined by X-ray crystallography. The complex $[Mn(L2)_2]ClO_4$, $C_{22}H_{20}N_6MnClO_6$, crystallizes in the monoclinic space group *C2/c* with four molecules in a unit cell of dimensions $a = 13.538(3)$ Å, $b = 13.754(3)$ Å, $c = 13.222(3)$ Å, and $\beta = 106.47(3)°$. The structure was solved by direct methods and refined by least-squares techniques to a final agreement factor of 0.0487 based on 1867 observed independent reflections. The structure of the $[Mn(L2)_2]^+$ cation reveals an axially compressed octahedral geometry at the manganese center. The complex $[Fe(L2)_2]ClO_4$, $C_{22}H_{20}N_6FeClO_6$, is isomorphous with the Mn complex, with $a = 13.423(3)$ Å, $b = 13.572(3)$ Å, $c = 13.371(3)$ Å, and $\beta = 107.89(3)°$. The structure was solved by direct methods and refined by least-squares techniques to a final agreement factor of 0.0521 based on 1723 observed independent reflections. The structure of the $[Fe(L2)_2]^+$ cation reveals a pseudooctahedral geometry for the iron center. The complex $[Ni(L1)_2](ClO_4)_2{\cdot}2CH_3CN$, $C_{32}H_{36}N_{12}NiCl_2O_8$, crystallizes in the orthorhombic space group *Pbca* with four molecules in a unit cell of dimensions $a = 12.252(2)$ Å, $b = 15.146(3)$ Å, and $c = 22.275(3)$ Å. The structure was solved by direct methods and refined by least-squares techniques to a final agreement factor of 0.0653 based on 802 observed independent reflections. The structure of the $[Ni(L1)_2]^{2+}$ cation reveals a pseudooctahedral geometry for the nickel center. Metal-assisted deamination/oxidation of the L1 ligand units during complexation is evident from the structures of the $Mn^{III}$ and $Fe^{III}$ complexes, but such oxidation is not observed with the $Ni^{II}$ ion. The room-temperature effective magnetic moments of 4.95 and 3.12 $\mu_B$ observed for the $Mn^{III}$ and $Ni^{II}$ complexes, respectively, indicate that they are high-spin $d^4$ and $d^8$ systems, whereas the value of 2.56 $\mu_B$ observed for the $Fe^{III}$ complex suggests that this is a low-spin $d^5$ complex. The electronic spectrum of the $Mn^{III}$ complex exhibits two weak spin-forbidden d−d transitions at 560 and 800 nm, whose presence is explained on the basis of axial compression of the $Mn^{III}$ center due to the expected Jahn−Teller effect. The $Mn^{III}$ and $Fe^{III}$ complexes exhibit a quasi-reversible or reversible one-electron oxidation at +1.155 and +1.450 V (*vs* Ag/AgCl), respectively, corresponding to the $M^{III} \leftrightarrow M^{IV}$ redox process.

## Introduction

High-oxidation-state manganese and iron complexes are important as synthetic models for the metal-active sites of the manganese- and iron-containing enzymes.[1,2] A number of redox processes, including water oxidation by the manganese-containing photosynthetic enzyme in higher plants and algae[3] and disproportionation of hydrogen peroxide by manganese and iron superoxide dismutases (Mn-SOD and Fe-SOD) in microorganisms,[4] are assumed to occur at the manganese or the iron active sites. The role of the metal ions in these and other biological redox processes has stimulated considerable interest in the design and synthesis of model complexes possessing physical and chemical properties similar to those of the enzymes.

We and others have synthesized a large number of such manganese and iron complexes and demonstrated the relevance of various types of oxo-bridged dinuclear manganese and iron chromophores in determining some of the properties of the biological systems.[5,6] We were also interested in the potential application of such complexes as catalysts in the oxidation of simple organic molecules.[5c,f] We have employed a variety of

[⊗] Abstract published in *Advance ACS Abstracts,* August 15, 1994.

(1) Vincent, J. B.; Olivier-Lilley, G. L.; Averill, B. A. *Chem. Rev.* **1990**, *90*, 1447 and references therein.
(2) Que, L., Jr.; True, A. E. *Prog. Inorg. Chem.* **1990**, *38*, 97.
(3) (a) Dismukes, D. C. *Photochem. Photobiol.* **1986**, *43*, 99. (b) dePaula, J. C.; Brudvig, G. W. *J. Am. Chem. Soc.* **1985**, *107*, 2643. (c) Renger, G.; Govindjee, T. *Photosynth. Res.* **1985**, *6*, 33. (d) Vincent, J. B.; Christou, G. *FEBS Lett.* **1986**, *207*, 250.
(4) (a) Kono, Y.; Fridovich, I. *J. Biol. Chem.* **1983**, *258*, 6015. (b) Kono, Y.; Fridovich, I. *J. Biol. Chem.* **1983**, *258*, 13646. (c) Stallings, W. C.; Pattridge, K. A.; Strong, R. K.; Ludwig, M. L. *J. Biol. Chem.* **1984**, *259*, 10695. (d) Salin, M. L.; Bridges, S. M. *Plant Physiol.* **1982**, *69*, 161.
(5) (a) Collins, M. A.; Hodgson, D. J.; Michelsen, K.; Pedersen, E. *J. Chem. Soc., Chem. Commun.* **1987**, 1659. (b) Goodson, P. A.; Hodgson, D. J. *Inorg. Chem.* **1989**, *28*, 3606. (c) Goodson, P. A.; Glerup, J.; Hodgson, D. J.; Michelsen, K.; Pedersen, E. *Inorg. Chem.* **1990**, *29*, 503. (d) Oki, A. R.; Glerup, J.; Hodgson, D. J. *Inorg. Chem.* **1990**, *29*, 2435. (e) Goodson, P. A.; Oki, A. R.; Glerup, J.; Hodgson, D. J. *Inorg. Chem.* **1990**, *112*, 6248. (f) Goodson, P. A.; Glerup, J.; Hodgson, D. J.; Michelsen, K.; Weihe, H. *Inorg. Chem.* **1991**, *30*, 4909. (g) Arulsamy, N.; Hodgson, D. J.; Glerup, J. *Inorg. Chim. Acta* **1993**, *209*, 61. (h) Arulsamy, N.; Goodson, P. A.; Hodgson, D. J.; Glerup, J.; Michelsen, K. *Inorg. Chim. Acta* **1994**, *209*, 21.
(6) (a) Sheats, J. E.; Czernuszewicz, R. S.; Dismukes, G. C.; Rheingold, A. L.; Petrouleas, V.; Stubbe, J.; Armstrong, W. H.; Beer, R. H.; Lippard, S. J. *J. Am. Chem. Soc.* **1987**, *109*, 1435. (b) Wieghardt, K.; Bossek, U.; Ventur, D.; Weiss, J. *J. Chem. Soc., Chem. Commun.* **1985**, 347. (c) Wieghardt, K.; Bossek, U.; Bonvoisin, J.; Beauvillain, P.; Girerd, J.-J.; Nuber, B.; Weiss, J.; Heinze, J. *Angew. Chem., Int. Ed. Engl.* **1986**, *25*, 1030. (d) Armstrong, W. H.; Lippard, S. J. *J. Am. Chem. Soc.* **1983**, *105*, 4837. (e) Wieghardt, K.; Pohl, K.; Gebert, W. *Angew. Chem., Int. Ed. Engl.* **1983**, *22*, 727. (f) Kurtz, D. M., Jr. *Chem. Rev.* **1990**, *90*, 585. (g) Vincent, J. B.; Christou, G. *Adv. Inorg. Chem.* **1990**, *33*, 197.

0020-1669/94/1333-4531$04.50/0 

tetradentate ligands for the synthesis of these complexes and have shown that the redox properties (and, hence, the catalytic behavior) of the bis(μ-oxo)diamanganese(IV/IV), -(IV/III), and -(III/III) complexes could be tuned by suitably modifying the ligand units. In this regard, we were interested in using the novel ligand (2-pyridyl)bis(2-pyridylamino)methane (L1) in the

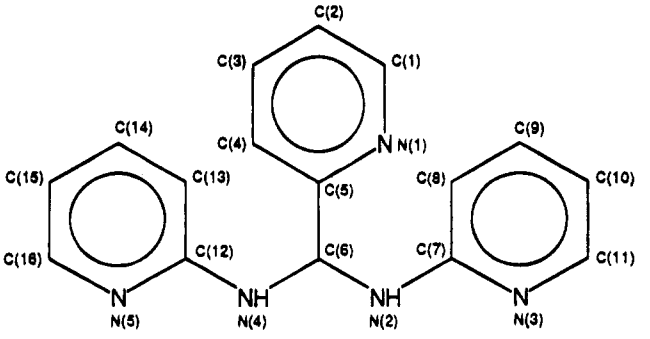


L1

synthesis of dinuclear manganese and iron complexes in higher oxidation states. The synthesis of this ligand has been reported by other workers,[7] but the coordination properties of the ligand have not been studied previously. In view of our experience with the polypyridyl ligands *N,N'*-bis(2-pyridylmethyl)ethane-1,2-diamine (bispicen) and tris(2-pyridylmethyl)amine (tmpa) and their analogues,[5] we expected that the ligand would form oxo-bridged dimanganese and diiron complexes under suitable experimental conditions. However, we find that in the presence of air L1 forms monomeric $Mn^{III}$ and $Fe^{III}$ complexes in which the ligand has undergone metal-assisted oxidative degradation. In order to ascertain the role of the $Mn^{III}$ and $Fe^{III}$ ions in the ligand oxidation, we have also synthesized a nickel(II) complex of the ligand in the presence of air, in which no ligand oxidation occurs. In this paper, we report the synthesis, characterization, and properties of these complexes.

## Experimental Section

**Materials.** 2-Pyridinecarboxaldehyde, 2-aminopyridine, $Mn(ClO_4)_2·6H_2O$, $Fe(ClO_4)_2·6H_2O$, and $Ni(ClO_4)_2·6H_2O$ were obtained from Aldrich. Elemental analyses were performed by Atlantic Microlab, Atlanta, GA.

*Caution! The perchlorate salts in this study are all potentially explosive and should be handled with care.*

**(2-Pyridyl)bis(2-pyridylamino)methane, L1.** The ligand was synthesized by a modified known procedure[7] as follows. A solution (50 mL) of 2-pyridinecarboxaldehyde (5.35 g, 0.05 mol) and 2-aminopyridine (9.41 g, 0.1 mol) in ethanol (95%) was refluxed for 6 h. The resultant yellow solution was allowed to cool slowly to room temperature. The colorless cubic crystals formed were isolated by filtration and washed with cold ethanol (95%, 10 mL). A second crop was obtained by further slow evaporation of the filtrate at room temperature. Yield: 11.5 g (83%).

**Bis[(2-pyridyl)(2-pyridylamino)methanolato]manganese(III) Perchlorate, $[Mn(L2)_2]ClO_4$.** To a suspension of L1 (0.555 g, 2 mmol) in ethanol (95%, 25 mL) was added $Mn(ClO_4)_2·6H_2O$ (0.362 g, 1 mmol) with stirring. The resultant yellow solution was stirred at room temperature for 10 min and filtered. The orange-red filtrate was allowed to stand at room temperature overnight. The yellow-brown crystals formed were filtered out, washed with ethanol (95%, 10 mL), and air-dried. Yield: 0.424 g (76%). Anal. Calcd for $C_{22}H_{20}N_6MnClO_6$: C, 47.62; H, 3.63; N, 15.15; Cl, 6.39. Found: C, 47.58; H, 3.64; N, 15.08; Cl, 6.52.

**Bis[(2-pyridyl)(2-pyridylamino)methanolato]iron(III) Perchlorate, $[Fe(L2)_2]ClO_4$.** To a suspension of L1 (0.555 g, 2 mmol) in ethanol (95%, 25 mL) was added $Fe(ClO_4)_2·6H_2O$ (0.363 g, 1 mmol) with stirring. The violet solution that formed immediately turned red after stirring for 1 h. The solution was filtered, and the filtrate was allowed to stand at room temperature overnight. The red crystals that formed were filtered out, washed with cold ethanol (95%, 5 mL), and air-dried. Yield: 0.220 g (40%). Anal. Calcd for $C_{22}H_{20}N_6FeClO_6$: C, 47.54; H, 3.63; N, 15.14; Cl, 6.38. Found: C, 47.64; H, 3.68; N, 15.05; Cl, 6.35.

**Bis[(2-pyridyl)bis(2-pyridylamino)methane]nickel(II) Perchlorate–Bis(acetonitrile), $[Ni(L1)_2](ClO_4)_2·2CH_3CN$.** To a suspension of L1 (0.555 g, 2 mmol) in acetonitrile (25 mL) was added $Ni(ClO_4)_2·6H_2O$ (0.366 g, 1 mmol) with stirring. The resultant wine-red solution was filtered, and the filtrate was allowed to stand at room temperature overnight. The violet-brown crystals that formed were filtered out, washed with cold ethanol (95%, 5 mL), and air-dried. Yield: 0.265 g (30%). Anal. Calcd for $C_{32}H_{36}N_{12}NiCl_2O_8$: C, 48.34; H, 4.06; N, 18.80; Cl, 7.93. Found: C, 48.16; H, 4.06; N, 18.63; Cl, 7.83.

**Physical Measurements.** Electronic absorption spectra were recorded on a Perkin-Elmer Lambda 9 spectrophotometer in acetonitrile solvent. Infrared spectra were recorded on a Perkin-Elmer 297 spectrophotometer as KBr disks. Magnetic susceptibility measurements were performed by the Faraday method on equipment described elsewhere.[8] The molar susceptibilities were corrected for ligand diamagnetism using Pascal's constants. Cyclic voltammograms were recorded on a BAS 100A electrochemical analyzer in acetonitrile, using a Pt-button working electrode, a Pt-wire auxiliary electrode, and a Ag/AgCl reference electrode. The solutions (0.001 M) contained tetraethylammonium perchlorate (0.1 M) as the supporting electrolyte.

**X-ray Structure Determination.** The structures of the complexes were determined at room temperature (295 K) on a Nicolet R3m/V diffractometer equipped with a molybdenum tube [$\lambda(K\alpha_1) = 0.709\,26$ Å; $\lambda(K\alpha_2) = 0.713\,54$ Å] and a graphite monochromator. Crystal data and experimental parameters are presented in Table 1. The data were corrected for Lorentz–polarization effects and absorption. The structures were solved by direct methods or Patterson techniques and refined by least-squares techniques; the programs used were from the SHELX-TL system.[9] The final values of the atomic positional parameters with their estimated standard deviations are listed in Tables 2–4.

**$[Mn(L2)_2]ClO_4$ and $[Fe(L2)_2]ClO_4$.** The complexes crystallize in the centrosymmetric monoclinic space group *C2/c* with four mononuclear cations in the unit cell. All hydrogen atoms were located in a

**Table 1.** Crystallographic and Data Collection Parameters for the Complexes

| | $[Mn(L2)_2]ClO_4$ | $[Fe(L2)_2]ClO_4$ | $[Ni(L1)_2](ClO_4)_2·2CH_3CN$ |
|---|---|---|---|
| formula | $C_{22}H_{20}N_6MnClO_6$ | $C_{22}H_{20}N_6FeClO_6$ | $C_{32}H_{36}N_{12}NiCl_2O_8$ |
| fw | 554.8 | 555.7 | 894.4 |
| size, $mm^3$ | 0.22 × 0.26 × 0.60 | 0.24 × 0.32 × 0.56 | 0.12 × 0.26 × 0.32 |
| $T$, K | 295 | 295 | 295 |
| space group | *C2/c* | *C2/c* | *Pbca* |
| $a$, Å | 13.538(3) | 13.423(3) | 12.252(2) |
| $b$, Å | 13.754(3) | 13.572(3) | 15.146(3) |
| $c$, Å | 13.222(3) | 13.371(3) | 22.275(4) |
| $\beta$, deg | 106.47(3) | 107.89(3) | 90 |
| $V$, $Å^3$ | 2361.1(9) | 2318.2(9) | 4133.5(13) |
| $Z$ | 4 | 4 | 4 |
| $d_{calc}$, Mg $m^{-3}$ | 1.561 | 1.592 | 1.437 |
| μ, $mm^{-1}$ | 0.724 | 0.819 | 0.664 |
| 2θ range, deg | 4–50 | 4–50 | 4–50 |
| NO[a] | 2723 | 2669 | 2697 |
| NO[$F>6\sigma(F)$] | 1867 | 1723 | 802 |
| $R$[b] | 0.0487 | 0.0521 | 0.0653 |
| $R_w$[c] | 0.0676 | 0.0681 | 0.0727 |
| $S$ | 1.41 | 1.72 | 1.59 |

[a] NO = number of observed reflections. [b] $R = \sum||F_o| - |F_c||/\sum|F_o|$. [c] $R_w = [\sum w(|F_o| - |F_c|)^2/\sum w|F_o|^2]^{1/2}$.

(7) Galverz, E.; Lorente, A.; Iriepa, I.; Florencio, F.; Garcia-Blanco, S. *J. Mol. Struct.* **1986**, *142*, 447.

(8) (a) Pedersen, E. *Acta Chem. Scand* **1972**, *26*, 333. (b) Josephsen, J.; Pedersen, E. *Inorg. Chem.* **1977**, *16*, 2534.

(9) Sheldrick, G. M. *SHELXTL-PLUS Crystallographic System*, Version 2; Nicolet XRD Corp.: Madison, WI, 1987.

**Table 2.** Atomic Coordinates ($\times 10^4$) and Equivalent Isotropic Displacement Coefficients ($Å^2 \times 10^3$) for $[Mn(L2)_2]ClO_4$

| | x | y | z | U(eq)[a] |
|---|---|---|---|---|
| Mn(1) | 0 | 900(1) | 2500 | 37(1) |
| N(1) | −1129(2) | −109(2) | 1608(2) | 43(1) |
| N(3) | −966(2) | 2048(2) | 1605(2) | 39(1) |
| O(1) | 871(2) | 840(2) | 1641(2) | 46(1) |
| C(1) | −1129(3) | −735(3) | 818(3) | 51(1) |
| C(2) | −1991(4) | −1259(3) | 323(3) | 59(2) |
| C(3) | −2883(4) | −1151(3) | 619(3) | 60(2) |
| C(4) | −2890(3) | −501(3) | 1422(3) | 50(1) |
| C(5) | −1999(3) | 6(2) | 1889(2) | 40(1) |
| C(6) | 1898(3) | 756(2) | 2239(3) | 42(1) |
| N(2) | −2316(2) | 1686(2) | 2318(3) | 49(1) |
| C(7) | −1887(2) | 2275(2) | 1736(2) | 38(1) |
| C(8) | −2414(3) | 3130(3) | 1287(3) | 50(1) |
| C(9) | −1965(4) | 3722(3) | 714(3) | 59(2) |
| C(10) | −1019(3) | 3481(3) | 567(3) | 61(2) |
| C(11) | −556(3) | 2648(3) | 1019(3) | 49(1) |
| Cl(1) | 5000 | 1712(2) | 2500 | 78(1) |
| O(2) | −5804(4) | 1225(7) | 1901(5) | 214(4) |
| O(3) | −4554(5) | 2308(6) | 1912(7) | 244(5) |

[a] Equivalent isotropic $U$ defined as one-third of the trace of the orthogonalized $U_{ij}$ tensor.

**Table 3.** Atomic Coordinates ($\times 10^4$) and Equivalent Isotropic Displacement Coefficients ($Å^2 \times 10^3$) for $[Fe(L2)_2]ClO_4$

| | x | y | z | U(eq)[a] |
|---|---|---|---|---|
| Fe(1) | 0 | 984(1) | 2500 | 35(1) |
| N(1) | −1034(3) | 2(3) | 1679(3) | 41(1) |
| N(3) | −927(2) | 2062(3) | 1659(2) | 36(1) |
| O(1) | −814(2) | 884(2) | 3407(2) | 44(1) |
| C(1) | −979(5) | −614(4) | 899(4) | 51(2) |
| C(2) | −1809(5) | −1206(3) | 396(4) | 60(2) |
| C(3) | −2702(5) | −1179(3) | 660(4) | 62(2) |
| C(4) | −2777(4) | −546(4) | 1443(4) | 52(2) |
| C(5) | −1921(3) | 35(3) | 1930(3) | 40(1) |
| C(6) | −1865(3) | 776(3) | 2794(3) | 44(2) |
| N(2) | −2288(3) | 1714(3) | 2356(3) | 48(1) |
| C(7) | −1869(3) | 2295(3) | 1765(3) | 37(1) |
| C(8) | −2414(4) | 3141(3) | 1283(4) | 49(2) |
| C(9) | −1975(5) | 3727(4) | 699(4) | 59(2) |
| C(10) | −1011(4) | 3474(4) | 586(4) | 57(2) |
| C(11) | −532(4) | 2650(3) | 1056(3) | 47(2) |
| Cl(1) | 5000 | 1660(2) | 2500 | 86(1) |
| O(2) | 5820(5) | 1187(8) | 3122(6) | 216(5) |
| O(3) | 5435(6) | 2283(8) | 1914(8) | 241(6) |

[a] Equivalent isotropic $U$ defined as one-third of the trace of the orthogonalized $U_{ij}$ tensor.

difference Fourier synthesis and their positions refined isotropically. All non-hydrogen atoms were refined anisotropically.

**$[Ni(L1)_2](ClO_4)_2 \cdot 2CH_3CN$.** The complex crystallizes in the centrosymmetric orthorhombic space group *Pbca* with four mononuclear cations in the unit cell. The hydrogen atoms were placed in calculated positions, while all the non-hydrogen atoms were refined anisotropically. As the crystal diffracted poorly, we had very few observable data, and hence the metrical parameters associated with this structure are of limited precision, but the present data do allow us to demonstrate the essential features of the structure.

## Results and Discussion

**Syntheses.** Previously, we demonstrated that 30% hydrogen peroxide solution can be used for the oxidation of manganese(II) complexes of tetradentate $N_4$ ligands in the synthesis of bis(μ-oxo)dimanganese(III/IV) and -(III/III) complexes.[5a-f] Hence, according to a similar procedure, an ethanolic solution of the ligand (2-pyridyl)bis(2-pyridylamino)methane (L1) was treated with a few drops of $H_2O_2$ solution with stirring. On cooling of the resultant dark-red solution, a yellow-brown precipitate was obtained. Subsequent experiments demonstrated that the same product could be obtained by aerial oxidation as yellow-brown

**Table 4.** Atomic Coordinates ($\times 10^4$) and Equivalent Isotropic Displacement Coefficients ($Å^2 \times 10^3$) for $[Ni(L1)_2](ClO_4)_2 \cdot 2CH_3CN$

| | x | y | z | U(eq)[a] |
|---|---|---|---|---|
| Ni(1) | 0 | 0 | 0 | 48(1) |
| N(1) | −520(14) | 994(11) | 596(6) | 52(7) |
| N(2) | −385(14) | −758(12) | 750(7) | 59(8) |
| N(5) | 1616(14) | 112(11) | 374(7) | 48(6) |
| C(1) | −911(16) | 1791(16) | 448(11) | 60(10) |
| C(2) | −1160(20) | 2410(16) | 874(15) | 89(12) |
| C(3) | −1019(21) | 2199(18) | 1478(13) | 102(14) |
| C(4) | −680(19) | 1352(17) | 1620(8) | 84(11) |
| C(5) | −437(18) | 774(14) | 1179(10) | 54(9) |
| C(6) | −65(26) | −163(16) | 1282(9) | 86(13) |
| C(7) | −572(16) | −1625(14) | 847(9) | 53(9) |
| C(8) | −434(17) | −2031(15) | 1424(9) | 71(10) |
| C(9) | −724(16) | −2904(17) | 1444(10) | 70(10) |
| C(10) | −1084(17) | −3386(13) | 955(11) | 72(10) |
| C(11) | −1273(16) | −2926(14) | 444(10) | 62(10) |
| N(3) | −1043(13) | −2059(11) | 378(7) | 49(7) |
| N(4) | 1057(22) | −260(11) | 1376(8) | 78(9) |
| C(12) | 1860(18) | −96(14) | 954(9) | 50(8) |
| C(13) | 2914(19) | −133(14) | 1169(9) | 60(9) |
| C(14) | 3717(20) | 95(14) | 774(11) | 86(10) |
| C(15) | 3477(21) | 264(15) | 173(9) | 79(12) |
| C(16) | 2450(21) | 255(10) | −7(10) | 57(8) |
| C(17) | 2262(28) | 2259(19) | 1921(11) | 220(23) |
| C(18) | 2132(29) | 2242(16) | 1312(14) | 123(15) |
| N(6) | 2016(22) | 2209(15) | 828(9) | 123(12) |
| Cl(1) | −1548(9) | 4586(5) | 2033(3) | 95(4) |
| O(1) | −1602(20) | 4457(10) | 1439(7) | 164(11) |
| O(2) | −1241(23) | 3948(11) | 2399(8) | 201(14) |
| O(3) | −2494(48) | 4743(37) | 2193(20) | 585(47) |
| O(4) | −1078(40) | 5254(19) | 2210(10) | 268(33) |

[a] Equivalent isotropic $U$ defined as one-third of the trace of the orthogonalized $U_{ij}$ tensor.

crystals by the procedure described above without the addition of the external oxidant $H_2O_2$. The product has been characterized by analytical and X-ray diffraction data to be a mononuclear $Mn^{III}$ complex, as will be described below (*vide infra*). The analogous $Fe^{III}$ complex was also synthesized by a similar procedure. Since the structural characterizations demonstrated that metal-assisted oxidation had occurred, an analogous reaction was also carried out with $Ni(ClO_4)_2 \cdot 6H_2O$. In this case, no ligand degradation took place and the $Ni^{II}$ complex $[Ni(L1)_2](ClO_4)_2 \cdot 2CH_3CN$ was isolated. In an effort to synthesize the $Mn^{II}$ and $Fe^{II}$ complexes of the ligand L1 (similar to the $Ni^{II}$ complex, $[Ni(L1)_2](ClO_4)_2 \cdot 2CH_3CN$), the syntheses were carried out under a nitrogen atmosphere. In each case, very air-sensitive pale yellow and violet-colored gummy solids, presumably the expected $Mn^{II}$ and $Fe^{II}$ complexes, respectively, were obtained. However, our efforts to obtain crystals of the complexes were unsuccessful. The formation of the $Mn^{III}$ and $Fe^{III}$ complexes in the presence of air further demonstrates that both the stability of the $Mn^{III}$ and $Fe^{III}$ oxidation states and their oxophilicity promote the ligand oxidation.

## Description of the Structures

**$[Mn(L2)_2]ClO_4$.** The structure consists of mononuclear $[Mn(L2)_2]^+$ cations and well-separated perchlorate anions. A view of the cation is shown in Figure 1. Selected bond distances and bond angles are listed in Table 5.

The manganese center is coordinated to two (2-pyridyl)(2-pyridylamino)methanolato ligand units through their pyridyl nitrogen atoms and the methanolato oxygen atoms. The geometry of the manganese center is distorted octahedral. As the manganese atom is located on a 2-fold axis, one half of the cation is symmetrically related to the other half. The four equatorial nitrogen atoms are nearly coplanar, the maximum deviation from the least-squares plane being 0.0853 Å; the manganese atom is constrained by symmetry to lie on this plane.

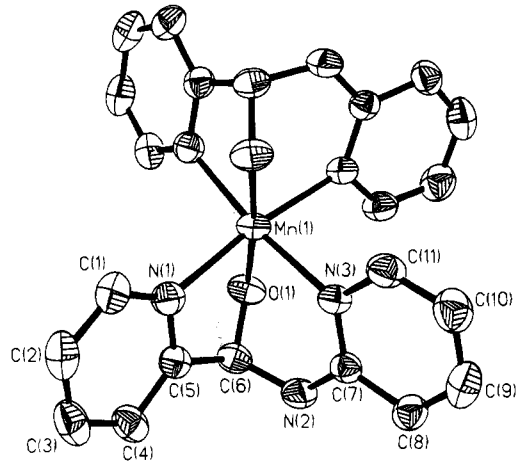


**Figure 1.** View of the $[Mn(L2)_2]^+$ cation in the structure of the perchlorate salt. Hydrogen atoms are omitted for clarity. Unlabeled atoms are related to labeled atoms by the horizontal crystallographic 2-fold axis passing through manganese.

**Table 5.** Bond Lengths (Å) and Angles (deg) for $[Mn(L2)_2]ClO_4$

Bond Lengths

| | | | |
|---|---|---|---|
| Mn(1)—N(1) | 2.152(3) | Mn(1)—N(3) | 2.174(3) |
| Mn(1)—O(1) | 1.856(3) | C(1)—N(1) | 1.354(5) |
| C(1)—C(2) | 1.370(6) | C(2)—C(3) | 1.378(8) |
| C(3)—C(4) | 1.391(6) | C(4)—C(5) | 1.378(5) |
| C(5)—C(6) | 1.524(5) | C(6)—N(2) | 1.452(4) |
| C(7)—N(2) | 1.356(5) | C(7)—N(3) | 1.344(4) |
| C(7)—C(8) | 1.415(5) | C(8)—C(9) | 1.367(6) |
| C(9)—C(10) | 1.388(7) | C(10)—C(11) | 1.360(5) |
| C(11)—N(3) | 1.354(5) | Cl(1)—O(2) | 1.331(6) |
| Cl(1)—O(3) | 1.380(9) | | |

Bond Angles

| | | | |
|---|---|---|---|
| N(1)—Mn(1)—N(3) | 86.9(1) | N(1)—Mn(1)—O(1) | 96.4(1) |
| N(3)—Mn(1)—O(1) | 95.0(1) | N(1)—Mn(1)—N(1A) | 99.7(1) |
| N(3)—Mn(1)—N(1A) | 172.3(1) | O(1)—Mn(1)—N(1A) | 80.2(1) |
| N(3)—Mn(1)—N(3A) | 86.8(1) | O(1)—Mn(1)—N(3A) | 88.7(1) |
| O(1)—Mn(1)—O(1A) | 174.8(2) | Mn(1)—N(1)—C(1) | 132.7(3) |
| Mn(1)—N(1)—C(5) | 108.4(2) | C(1)—N(1)—C(5) | 118.7(3) |
| Mn(1)—N(3)—C(7) | 122.4(2) | Mn(1)—N(3)—C(11) | 118.3(2) |
| C(7)—N(3)—C(11) | 118.6(3) | Mn(1)—O(1)—C(6) | 111.2(2) |
| N(1)—C(1)—C(2) | 121.1(4) | C(1)—C(2)—C(3) | 120.2(4) |
| C(2)—C(3)—C(4) | 118.9(4) | C(3)—C(4)—C(5) | 118.2(4) |
| N(1)—C(5)—C(4) | 122.8(3) | N(1)—C(5)—C(6A) | 113.1(3) |
| C(4)—C(5)—C(6A) | 124.1(3) | O(1)—C(6)—C(5A) | 110.2(3) |
| O(1)—C(6)—N(2A) | 111.6(3) | C(5A)—C(6)—N(2A) | 110.5(3) |
| C(7)—N(2)—C(6A) | 125.0(3) | N(3)—C(7)—N(2) | 119.8(3) |
| N(3)—C(7)—C(8) | 121.0(3) | N(2)—C(7)—C(8) | 119.2(3) |
| C(7)—C(8)—C(9) | 118.4(4) | C(8)—C(9)—C(10) | 120.6(4) |
| C(9)—C(10)—C(11) | 117.9(4) | N(3)—C(11)—C(10) | 123.5(4) |
| O(2)—Cl(1)—O(3) | 112.2(4) | O(2)—Cl(1)—O(2A) | 119.6(7) |
| O(3)—Cl(1)—O(2A) | 102.7(4) | O(3)—Cl(1)—O(3A) | 107.2(7) |

The (axial) Mn—O bond distances of 1.856(3) Å are relatively short, while the (equatorial) Mn—N bond distances of 2.152(3) and 2.174(3) Å are long when compared to those of other $Mn^{III}$ complexes,[10b,d,11b-d] revealing an axially compressed octahedral geometry for the cation. The distortion may be attributed to the Jahn–Teller effect expected for the high-spin $d^4$ $Mn^{III}$ ion. However, the observation of axial compression in this complex is unusual, since most of the other known $Mn^{III}$ complexes exhibit axial elongation.[10,11]

**Table 6.** Bond Lengths (Å) and Angles (deg) for $[Fe(L2)_2]ClO_4$

Bond Lengths

| | | | |
|---|---|---|---|
| Fe(1)—N(1) | 1.993(3) | Fe(1)—N(3) | 2.024(3) |
| Fe(1)—O(1) | 1.870(3) | C(1)—N(1) | 1.357(6) |
| C(1)—C(2) | 1.371(8) | C(2)—C(3) | 1.351(10) |
| C(3)—C(4) | 1.381(8) | C(4)—C(5) | 1.381(6) |
| C(5)—C(6) | 1.517(6) | C(5)—N(1) | 1.333(6) |
| C(6)—O(1) | 1.405(5) | C(6)—N(2) | 1.442(6) |
| C(7)—C(8) | 1.406(6) | C(7)—N(2) | 1.355(6) |
| C(7)—N(3) | 1.352(5) | C(8)—C(9) | 1.370(8) |
| C(9)—C(10) | 1.391(9) | C(10)—C(11) | 1.346(7) |
| C(11)—N(3) | 1.353(6) | Cl(1)—O(2) | 1.324(7) |
| Cl(1)—O(3) | 1.397(11) | | |

Bond Angles

| | | | |
|---|---|---|---|
| N(1)—Fe(1)—N(3) | 88.4(1) | N(1)—Fe(1)—O(1) | 82.1(1) |
| N(3)—Fe(1)—O(1) | 91.7(1) | N(1)—Fe(1)—N(1A) | 96.0(2) |
| N(3)—Fe(1)—N(1A) | 174.3(1) | O(1)—Fe(1)—N(1A) | 92.4(1) |
| N(3)—Fe(1)—N(3A) | 87.3(2) | O(1)—Fe(1)—N(3A) | 94.2(1) |
| N(1)—Fe(1)—O(1A) | 92.4(1) | O(1)—Fe(1)—O(1A) | 171.7(2) |
| Fe(1)—N(1)—C(1) | 129.9(4) | Fe(1)—N(1)—C(5) | 111.3(3) |
| C(1)—N(1)—C(5) | 118.6(4) | Fe(1)—N(3)—C(7) | 123.1(3) |
| Fe(1)—N(3)—C(11) | 118.1(3) | C(7)—N(3)—C(11) | 118.4(3) |
| Fe(1)—O(1)—C(6) | 108.1(3) | N(1)—C(1)—C(2) | 120.7(6) |
| C(1)—C(2)—C(3) | 120.6(5) | C(2)—C(3)—C(4) | 119.5(5) |
| C(3)—C(4)—C(5) | 117.9(5) | N(1)—C(5)—C(4) | 122.7(4) |
| N(1)—C(5)—C(6) | 112.0(3) | C(4)—C(5)—C(6) | 125.2(5) |
| O(1)—C(6)—C(5) | 108.7(4) | O(1)—C(6)—N(2) | 110.1(3) |
| C(5)—C(6)—N(2) | 110.8(4) | C(6)—N(2)—C(7) | 124.7(4) |
| N(3)—C(7)—N(2) | 119.6(3) | N(3)—C(7)—C(8) | 121.0(4) |
| N(2)—C(7)—C(8) | 119.4(4) | C(7)—C(8)—C(9) | 118.7(5) |
| C(8)—C(9)—C(10) | 119.8(5) | C(9)—C(10)—C(11) | 118.8(5) |
| N(3)—C(11)—C(10) | 123.3(5) | O(2)—Cl(1)—O(3) | 103.7(5) |
| O(2)—Cl(1)—O(2A) | 122.0(9) | O(3)—Cl(1)—O(2A) | 110.6(5) |
| O(3)—Cl(1)—O(3A) | 105.4(9) | | |

There is a crystallographic 2-fold axis passing through the chlorine atom of the perchlorate anion, relating the oxygen atoms on one side to those on the other. The perchlorate is well-behaved with Cl—O bond distances of 1.331(6) and 1.381(9) Å and O—Cl—O bond angles in the range 102.7(4)–119.9(7)°. These metrical parameters are similar to those reported in earlier studies.[12]

**$[Fe(L2)_2]ClO_4$.** The $Fe^{III}$ complex is isomorphous with the $Mn^{III}$ complex described above, the structure again consisting of mononuclear $[Fe(L2)_2]^+$ cations and well-separated perchlorate anions. Necessarily, the geometric features of the complex are substantially similar to those of the manganese complex, but as can be seen from Table 6, any distortion from octahedral geometry is much smaller in the case of this low-spin $d^5$ $Fe^{III}$ ion.

**$[Ni(L1)_2](ClO_4)_2{\cdot}2CH_3CN$.** The structure consists of $[Ni(L1)]^{2+}$ cations, perchlorate anions, and uncoordinated acetonitrile molecules. A view of the cation is shown in Figure 2. Selected bond distances and angles are listed in Table 7. As already mentioned, because of the paucity of data, the metrical parameters here are less precisely determined than for the two previous structures, but the essential features of the structure are well characterized.

The geometry at the nickel center is approximately octahedral, with two ligand units binding the metal center. The ligand (2-pyridyl)bis(2-pyridylamino)methane (L1) binds the metal center through two of the three pyridyl nitrogen atoms and one of the two secondary amine nitrogen atoms. This mode of ligand

(10) (a) Streetz, B. R.; Day, R. O.; Marianelli, R. S.; Day, V. W. *Inorg. Chem.* **1979**, *18*, 1847. (b) Stults, J.; Marianelli, R. S.; Day, V. W. *Inorg. Chem.* **1979**, *18*, 1853. (c) Stein, J.; Fackler, J. P., Jr.; McClieme, G. J.; Fee, J. A.; Chan, L. T. *Inorg. Chem.* **1979**, *18*, 3511. (d) Wieghardt, K.; Bossek, U.; Nuber, B.; Weiss, J. *Inorg. Chim. Acta* **1987**, *126*, 39.

(11) (a) Bonadies, J. A.; Kirk, M. L.; Lah, M. S.; Kessissoglou, D. P.; Hatfield, W. E.; Pecoraro, V. L. *Inorg. Chem.* **1989**, *28*, 2044. (b) Auerback, U.; Eckert, U.; Wieghardt, K.; Nuber, B.; Weiss, J. *Inorg. Chem.* **1990**, *29*, 938. (c) Oki, A. R.; Hodgson, D. J. *Inorg. Chim. Acta* **1990**, *170*, 65. (d) Bertoncello, K.; Fallon, G. D.; Murray, K. *Inorg. Chim. Acta* **1990**, *174*, 57. (e) Neves, A.; Erthal, S. M. D.; Vencato, I.; Ceccato, A. S.; Mascarenhas, Y. P.; Nascimento, O. R.; Horner, M.; Batista, A. A. *Inorg. Chem.* **1992**, *31*, 4749.

(12) See, for example: Goodson, P. A.; Glerup, J.; Hodgson, D. J.; Michelsen, K.; Rychlewska, U. *Inorg. Chem.* **1994**, *33*, 359 and references therein.

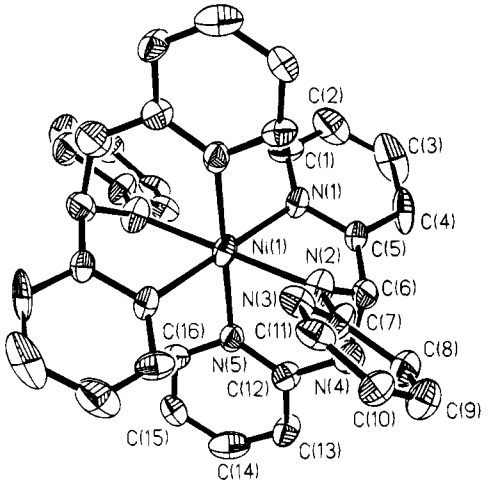


**Figure 2.** View of the $[Ni(L1)_2]^{2+}$ cation in the structure of the perchlorate salt. Hydrogen atoms are omitted for clarity. Unlabeled atoms are related to labeled atoms by the crystallographic inversion center at Ni.

**Table 7.** Selected Bond Lengths (Å) and Angles (deg) for $[Ni(L1)_2](ClO_4)_2 \cdot 2CH_3CN$

| Bond Lengths | | | |
|---|---|---|---|
| Ni(1)—N(1) | 2.106(16) | Ni(1)—N(2) | 2.081(16) |
| Ni(1)—N(5) | 2.155(16) | N(1)—C(1) | 1.341(29) |
| N(1)—C(5) | 1.345(26) | N(2)—C(6) | 1.539(27) |
| N(2)—C(7) | 1.351(28) | N(3)—C(7) | 1.360(26) |
| N(3)—C(11) | 1.351(27) | N(4)—C(6) | 1.398(41) |
| N(4)—C(12) | 1.384(31) | N(5)—C(12) | 1.363(25) |
| N(5)—C(16) | 1.346(29) | | |

| Bond Angles | | | |
|---|---|---|---|
| N(1)—Ni(1)—N(2) | 79.6(6) | N(1)—Ni(1)—N(5) | 88.7(6) |
| N(2)—Ni(1)—N(5) | 86.6(6) | N(1)—Ni(1)—N(1A) | 180.0(1) |
| N(2)—Ni(1)—N(1A) | 100.4(6) | N(5)—Ni(1)—N(1A) | 91.3(6) |
| N(1)—Ni(1)—N(2A) | 100.4(6) | N(2)—Ni(1)—N(2A) | 180.0(1) |
| N(5)—Ni(1)—N(2A) | 93.4(6) | N(1)—Ni(1)—N(5A) | 91.3(6) |
| N(2)—Ni(1)—N(5A) | 93.4(6) | N(5)—Ni(1)—N(5A) | 180.0(1) |

binding leads to the formation of five- and six-membered chelate rings. Although ligand L1 contains five nitrogen donors, the use of more than three as donors to the metal center would lead to the formation of four-membered chelate rings. Specifically, if four-membered rings are to be avoided, only one of the amine nitrogen atoms [N(2) and N(4)] can be used, and the nitrogen atom of the terminal pyridyl group adjacent to the coordinated amine nitrogen atom cannot be used. Consequently, the arrangement depicted in Figure 2 is the only possible unique combination of nitrogen donors; however, in addition to the present *fac* isomer, there could be a *mer* isomer which we have not observed. In the present case, the nickel atom is located on a crystallographic inversion center, and one half of the cation is symmetrically related to the other half. The equatorial and axial Ni—N bond distances and the associated N—Ni—N bond angles (Table 7) are normal and are consistent with those of other $NiN_6$ complexes.[13] The most notable feature of the ligand geometry, presumably the result of the coordination mode described above, is that the C—N bond lengths from the central carbon atom [C(6)] to the amine nitrogen atoms are unequal, the C(6)—N(2) bond of 1.54(4) Å to the coordinated nitrogen atom being significantly longer than the C(6)—N(4) distance of 1.40(4) Å.

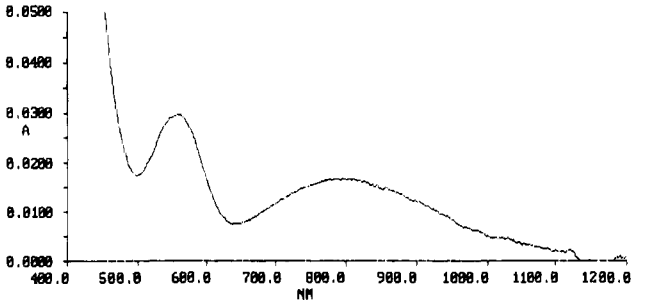


**Figure 3.** Electronic spectrum of the $Mn^{III}$ complex $[Mn(L2)_2]ClO_4$ in acetonitrile.

The perchlorate anions are somewhat disordered with the Cl—O distances in the range 1.230(34)—1.337(17) Å and the O—Cl—O bond angles in the range 100.8(33)—121.2(12)°. The acetonitrile molecules are well separated from the cation.

From a comparison of the structures of the $Mn^{III}$, $Fe^{III}$, and $Ni^{II}$ complexes the following conclusions may be drawn: Under an inert atmosphere, the ligand L1 very probably binds the $Mn^{II}$ and $Fe^{II}$ ions in a coordination mode analogous to that seen in the $Ni^{II}$ complex (Figure 2), since this is the only available mode that does not involve significant steric strain. In the presence of air, the $Mn^{II}$ and $Fe^{II}$ complexes undergo oxidation with concomitant deamination/oxidation of the ligand units. The long N(2)—C(6) bond distance observed in the $Ni^{II}$ complex clearly demonstrates that this bond is weak and subject to cleavage, which supports the suggestion that the stable and oxophilic $Mn^{III}$ and $Fe^{III}$ ions promote the oxidative degradation of the ligand units during complexation.

**Magnetic Susceptibility.** The room-temperature magnetic moments of the $[Mn(L2)_2]ClO_4$, $[Fe(L2)_2]ClO_4$, and $[Ni(L1)_2](ClO_4)_2 \cdot 2CH_3CN$ complexes are 4.95, 2.56, and 3.12 $\mu_B$, respectively. These data indicate that the $Mn^{III}$ and $Ni^{II}$ complexes are high-spin $d^4$ and $d^8$ systems, respectively, whereas the $Fe^{III}$ complex is low spin. The observed magnetic moment of the $Fe^{III}$ complex is considerably larger than the spin-only value of 1.73 $\mu_B$ for one unpaired electron, but this result is attributable to the presence of orbital angular momentum for this $^2T_{2g}$ ($O_h$) ground term ion.[14]

**IR and Electronic Spectra.** The IR spectra of the complexes $[Mn(L2)_2]ClO_4$ and $[Fe(L2)_2]ClO_4$ exhibit sharp absorption maxima at 3347 and 3352 $cm^{-1}$, respectively, indicating the presence in the ligand L2 of the N—H group. No other absorption maximum in the region 3400—3600 $cm^{-1}$ was observed, indicating the absence of O—H groups in this ligand.

The electronic absorption spectra were measured for the complexes in acetonitrile solvent. The spectra of all the complexes in the UV region display a strong absorption due to a ligand-related transition at *ca.* 290 nm. The $Mn^{III}$ complex exhibits a shoulder of moderate intensity at *ca.* 460 nm and two well-defined, weak bands at 560 and 800 nm with $\epsilon = 25$ and 14 $M^{-1}$ $cm^{-1}$, respectively, as shown in Figure 3. The electronic spectrum of the $Mn^{III}$ complex is different from those of other known $Mn^{III}$ complexes, which in general exhibit a ligand to metal charge transfer band in the range 380—560 nm and, in some cases, a d—d transition ($^5E_{2g} \rightarrow {}^5T_g$) in the range 560—660 nm.[11b,d,15] Although the shoulder at 460 nm could analogously be assigned to a transition of ligand → metal charge transfer, the two weak absorptions in the visible region require additional explanation. As described earlier, the present complex possesses axially compressed octahedral geometry unlike the other $Mn^{III}$ complexes, which exhibit axial elongation.

(13) (a) Zomba, L. J.; Margulis, T. N. *Inorg. Chim. Acta* **1980**, *45*, L264. (b) Thom, V. J.; Boeyens, J. C. A.; McDougall, G. J.; Hancock, R. D. *J. Am. Chem. Soc.* **1984**, *106*, 3198. (c) Wieghardt, K.; Schoffmann, E.; Nuber, B.; Weiss, J. *Inorg. Chem.* **1986**, *25*, 4877. (d) Bushnell, G. W.; Fortier, D. G.; McAuley, A. *Inorg. Chem.* **1988**, *27*, 2676.

(14) Figgis, B. N.; Lewis, J. *Prog. Inorg. Chem.* **1964**, *6*, 37.

(15) Patch, M. G.; Simolo, K. P.; Carrano, C. J. *Inorg. Chem.* **1982**, *21*, 2972.

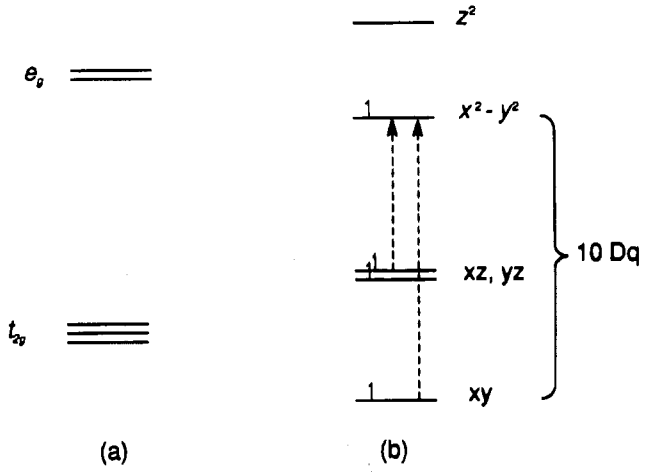


**Figure 4.** Orbital energy diagram for an octahedral complex (a) and an axially compressed high-spin $d^4$ complex (b). The dashed lines indicate the two spin-forbidden d → d transitions observed in the spectrum of the $Mn^{III}$ complex.

In the axially compressed octahedral environment, the $t_{2g}$ and $e_g$ orbitals will further split with lowering of the $xy$ and $x^2 - y^2$ orbitals.[16] As a result, as is shown in Figure 4, there can be two spin-allowed d−d transitions, *viz.*, $xy \rightarrow z^2$ and $xz$ $(yz) \rightarrow z^2$, and two spin-forbidden transitions, *viz.*, $xy \rightarrow x^2 - y^2$ and $xz$ $(yz) \rightarrow x^2 - y^2$ (the $xz$ and $yz$ orbitals are degenerate). The low $\epsilon$ values observed for the two bands at 560 and 800 nm indicate that they are probably due to the two spin-forbidden transitions, $xy \rightarrow x^2 - y^2$ and $xz$ $(yz) \rightarrow x^2 - y^2$, respectively. In that case, the former transition should be equal to the crystal field splitting energy, $10Dq$, and the difference between the energies of the two transitions (4170 $cm^{-1}$) should be equal to the energy of splitting of the $t_{2g}$ orbitals. In this model, the transition $xy \rightarrow x^2 - y^2$ at 560 nm corresponds to an energy separation of 17 860 $cm^{-1}$, in agreement with the $10Dq$ values of 17 800 and 17 900 $cm^{-1}$ determined for $[Mn^{III}F_6]^{3-}$ and $[Mn(acac)_3]$,[17] respectively, supporting the above assignment. We assume that the two spin-allowed transitions (of higher energy) are obscured by the strong charge transfer band at 460 nm.

The $Fe^{III}$ complex also exhibits a shoulder at 460 nm attributable to a charge transfer transition of ligand → metal, and no other band is observed in the visible region; if we again assume that the spin-allowed d−d transitions are obscured by the charge transfer band, this is consistent with the assignment of the complex as low-spin $d^5$ deduced from the observed magnetic moment (*vide supra*).

No absorption could be observed in the visible region of the $Ni^{II}$ complex. Although high-spin $Ni^{II}$ complexes, in general, exhibit weak absorptions in the visible region attributable to d−d transitions,[13] in the present case the limited solubility of the complex presumably combines with their anticipated low intensity to preclude our observing them.

**Electrochemistry.** Cyclic voltammograms of the complexes were recorded in acetonitrile in the potential range −1.5 to +1.8 V *vs* Ag/AgCl reference electrode. As is shown in Figure 5A, the $Mn^{III}$ complex exhibits a quasi-reversible one-electron oxidation at +1.155 V ($\Delta E_p$ = 70 mV) corresponding to the $Mn^{III} \leftrightarrow Mn^{IV}$ redox process,[11e] and an irreversible reduction at −0.320 V. The $Fe^{III}$ complex (Figure 5B) exhibits very similar electrochemical behavior, with a reversible one-electron oxidation couple at +1.450 V ($\Delta E_p$ = 60 mV), attributable to the $Fe^{III} \leftrightarrow Fe^{IV}$ redox process, and an irreversible reduction at

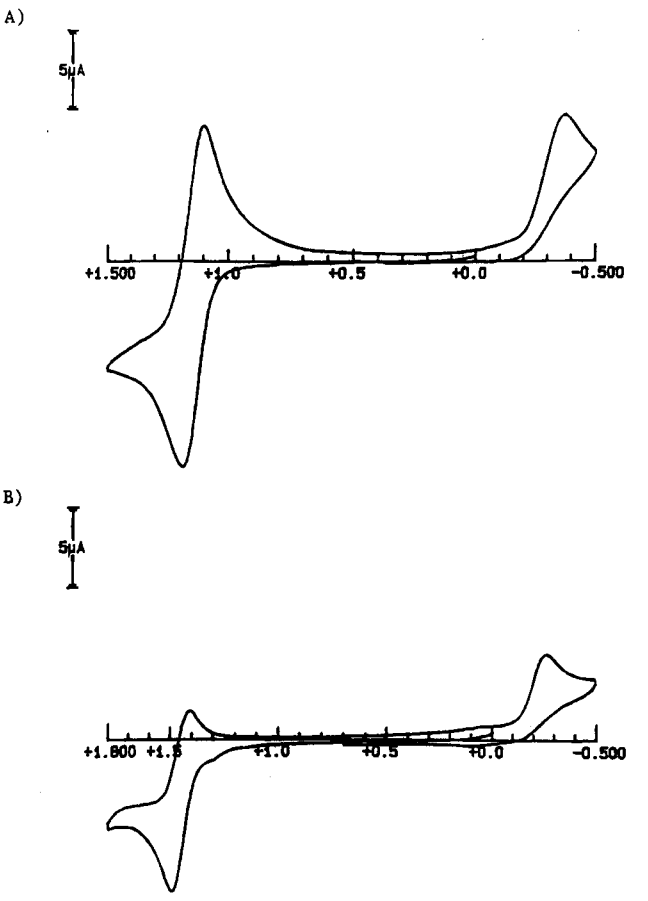


**Figure 5.** Cyclic voltammograms recorded in acetonitrile with 0.1 M TEAP supporting electrolyte of (A) the $Mn^{III}$ complex $[Mn(L2)_2]ClO_4$ and (B) the $Fe^{III}$ complex $[Fe(L2)_2]ClO_4$ (scan rate 100 mV/s; potentials recorded vs Ag/AgCl reference electrode).

−0.255 V. The irreversible reduction peaks observed for both complexes indicate that the analogous $Mn^{II}$ and $Fe^{II}$ complexes are unstable, consistent with the exclusive formation of the $Mn^{III}$ and $Fe^{III}$ complexes in the synthetic reactions. The $Ni^{II}$ complex exhibits an irreversible oxidation peak at +1.440 V and an irreversible reduction at −0.690 V, indicating immediate decomposition of the electrogenerated species, as expected for this complex with a cleavable C−N bond as described above.

## Conclusions

The ligand (2-pyridyl)bis(2-pyridylamino)methane (L1) undergoes metal-assisted deamination/oxidation in the presence of the oxophilic $Mn^{III}$ and $Fe^{III}$ ions, forming novel mononuclear complexes, but forms the expected bis-ligated complex with the $Ni^{II}$ ion. The $Mn^{III}$ complex possesses an axially compressed octahedral geometry due to Jahn−Teller-distorted high-spin $d^4$ $Mn^{III}$ ion, which leads to the observation of two weak spin-forbidden d−d transitions in the visible region of the electronic spectrum. The $Mn^{III}$ and the $Fe^{III}$ complexes exhibit quasi-reversible or reversible one-electron oxidation processes at high redox potentials. Our current research is aimed at studying the ligation properties of L1 in the presence of other biologically active transition metal ions such as copper.

**Acknowledgment.** This work was supported by the National Science Foundation through Grant No. CHE-9007607.

**Supplementary Material Available:** Tables S1-S3 (hydrogen atom parameters) and S4-S6 (anisotropic thermal parameters) for the three structures (7 pages). For ordering information, consult any current masthead page. Listings of observed and calculated structure amplitudes are available from D.J.H. on request.

(16) Huheey, J. E. *Inorganic Chemistry: Principles of Structure and Reactivity*, 3rd ed.; Harper & Row: New York, 1983; p 397.
(17) Lever, A. B. P. *Inorganic Electronic Spectroscopy*, 2nd ed.; Elsevier: New York, 1986; p 435.